Ab initio studies of electron correlation and Gaunt interaction effects in the boron isoelectronic sequence using coupled-cluster theory

Narendra Nath Dutta* and Sonjoy Majumder

Department of Physics and Meteorology, Indian Institute of Technology—Kharagpur, Kharagpur 721302, India

(Received 23 November 2011; revised manuscript received 25 January 2012; published 16 March 2012)

In this paper, we study electron correlation and Gaunt interaction effects in ionization potentials (IPs) and hyperfine constants A of $2p\,^2P_{1/2}$ and $2p\,^2P_{3/2}$ states along with fine structure splitting (FSS) between them for the boron isoelectronic sequence using the relativistic coupled-cluster method. The range of atomic number z is taken from 8 to 21. The Gaunt contributions can be calculated at both the Dirac-Fock and the coupled-cluster levels from our presentation. Calculated IPs and FSS are compared with the results of the National Institute of Standards and Technology. Important correlation contributions like the core correlation, core polarization, and pair correlation effects are studied for hyperfine constants A. Many distinct features of the correlation and relativistic effects are observed in these studies.

DOI: 10.1103/PhysRevA.85.032512 PACS number(s): 32.10.−f

I. INTRODUCTION

Research in isoelectronic sequences of lighter atoms has been a subject of recent interest for study of various atomic properties of low-lying atomic states and the transitions between them [1–3]. Accurate estimations of these properties require correlation corrections with the Breit and quantum electrodynamic (QED) effects [4]. However, individual studies of all these effects are necessary to realize the relative strengths between them with increasing atomic number for different isoelectronic sequences. To implement these effects in different many-body theories, a suitable form of matrix elements of their operators is necessary. From our literature survey, we found a number of such formulations for the Breit operator [5–9]. However, in our work, we have implemented the Gaunt interaction, which is the magnetic part of the Breit interaction [9] and is considered to be an order of magnitude larger than the other part, called the retardation part [5]. Hence, the Gaunt interaction is assumed to provide a useful approximation to the Breit interaction [5]. The matrix element of the Gaunt operator is reformulated to add with the matrix element of the Coulomb operator in a self-consistent approach at both the Dirac-Fock (DF) and the coupled-cluster (CC) level of calculations.

In recent years, a number of theoretical calculations have been performed on the boron isoelectronic sequence considering the Breit interaction in the atomic Hamiltonian [3,4,10–23]. These calculations have been performed using different many-body approaches like the configuration-interaction technique [3,10,22], multiconfiguration DF method [4,11,12], weakest bound electron potential model theory [23], relativistic multireference configuration-interaction technique [13–16], multiconfiguration Hartree-Fock method [17], and relativistic many-body perturbation theory [18–21]. Eliav *et al.* have implemented the Breit interaction in the CC theory and treated only four members of this sequence to calculate the ionization potentials (IPs) and fine structure splitting (FSS) [24]. Recently, relativistic CC (RCC) calculations of this sequence were performed by Nataraj *et al.* [25] for Mg VIII, Si X, and S XII. They performed RCC calculations on different transition properties among some low-lying states of these ions on the basis of the Dirac-Coulomb Hamiltonian. However, the improvement in the fine structures due to the inclusion of relativistic effects, which was pointed out by Eliav *et al.* [26], is highlighted here for these three elements.

Isoelectronic sequences are also very useful for studying the trends of relativistic and different correlation effects in hyperfine properties of different ions [27]. Panigrahy *et al.* investigated the different correlation mechanisms on the magnetic dipole hyperfine constants (A) of Li-like systems using the relativistic linked-cluster many-body perturbation theory [27]. As members of the boron isoelectronic sequence, the hyperfine constants of C II, N III, and O IV were calculated by Jönsson *et al.* [28]. QED and interelectronic interaction corrections in hyperfine properties were analyzed by Oreshkina *et al.* using the large-scale configuration-interaction Dirac-Fock-Sturm method for a few members of this sequence [29].

The purpose of the present paper is to analyze correlation and Gaunt effects in the calculations of IPs, hyperfine constants A of $2p\,^2P_{1/2}$ and $2p\,^2P_{3/2}$ states, and FSS between them for boron-like systems using the RCC approach. Systematic investigations of both these effects with increasing atomic number provide comparative information about their contributions in the calculations of these properties. Gaunt contributions at both the DF and the CC levels of calculations have been explicitly studied to test the correlation effects on these. Our final calculated results for IPs and FSS, including correlation and Gaunt effects, are compared with the results of the National Institute of Standards and Technology (NIST) [30]. Graphical variations of these effects are shown with increasing atomic number. The RCC method, applied in these calculations, consist of single, double, and partial triple excitations [31]. Different types of correlation effects like the core correlation, pair correlation, and core polarization in the hyperfine constants are plotted to observe their variations with regard to (w.r.t.) Z.

*narendranathdutta7@gmail.com

 ©2012 American Physical Society

II. THEORY

A. Matrix element of the Gaunt interaction operator

The Breit interaction, introduced by Breit [32], is the first relativistic correction of the Coulomb interaction. The frequency-independent form of the Breit interaction between two electrons, indicated by 1 and 2, is given by

$$H_B = -\frac{\vec{\alpha_1}\cdot\vec{\alpha_2}}{r_{12}} + \frac{1}{2}\left[\frac{\vec{\alpha_1}\cdot\vec{\alpha_2}}{r_{12}} - \frac{(\vec{\alpha_1}\cdot\vec{r_{12}})(\vec{\alpha_2}\cdot\vec{r_{12}})}{r_{12}^3}\right], \tag{2.1}$$

where α_1 and α_2 are the corresponding Dirac matrices and r_{12} is the distance of separation between the two electrons [33]. The overall Breit interaction is contributed by the magnetic part, called the Gaunt interaction [34], as stated earlier, represented by the first term in Eq. (2.1), and the other part, which includes the retardation effect, called the retardation part, represented by the remainder of this equation.

Including the Gaunt interaction with the Coulomb interaction, the atomic Hamiltonian of an N-electron system is written in the form

$$H = \sum_{i=1}^{N}\left[c\,\vec{\alpha_i}\cdot\vec{p_i} + (\beta_i - 1)\,c^2 + V_{\rm nuc}(r_i) + \sum_{j>i}^{N}\left(\frac{1}{r_{ij}} - \frac{\vec{\alpha_i}\cdot\vec{\alpha_j}}{r_{ij}}\right)\right]. \tag{2.2}$$

The Gaunt interaction can be expanded in terms of irreducible tensor operators [7,9],

$$B_g = \sum_{\nu,L}(-1)^{\nu+L}V_\nu(1,2)[\mathbf{X}^{[(1\nu)L]}(1).\mathbf{X}^{[(1\nu)L]}(2)], \tag{2.3}$$

where $\nu = L-1$, L, or $L+1$ and $\mathbf{X}^{[(1\nu)L]}(1) = [\boldsymbol{\alpha}_1\mathbf{C}^{(\nu)}(1)]^{(L)}$ [7]. In the long-wavelength approximation [7],

$$V_\nu(1,2) = \frac{r_<^\nu}{r_>^{\nu+1}}, \tag{2.4}$$

where $r_< = \min(r_1,r_2)$ and $r_> = \max(r_1,r_2)$.

Knowledge of the general two-electron matrix element of the Gaunt operator is necessary to include this effect in the CC theory, which is derived from Ref. [7] and is given as follows:

$$\begin{aligned}\langle A_1B_2|B_g|C_1D_2\rangle &= \langle A_1B_2|\sum_{\nu,L}(-1)^{\nu+L}V_\nu(1,2)[\mathbf{X}^{[(1\nu)L]}(1).\mathbf{X}^{[(1\nu)L]}(2)]|C_1D_2\rangle \\ &= \sum_{L,M}(-1)^{j_A-m_A+j_B-m_B+L-M}\begin{pmatrix} j_A & L & j_C \\ -m_A & M & m_C\end{pmatrix} \\ &\quad\times\begin{pmatrix} j_B & L & j_D \\ -m_B & -M & m_D\end{pmatrix}X^L(ABCD).\end{aligned} \tag{2.5}$$

Here the effective interaction strength, $X^L(ABCD)$, is written in the following form:

$$\begin{aligned}X^L(ABCD) &= (-1)^{j_A+j_B+L+1}\sqrt{(2j_A+1)(2j_B+1)(2j_C+1)(2j_D+1)}\begin{pmatrix} j_A & L & j_C \\ \frac{1}{2} & 0 & -\frac{1}{2}\end{pmatrix}\begin{pmatrix} j_B & L & j_D \\ \frac{1}{2} & 0 & -\frac{1}{2}\end{pmatrix} \\ &\quad\times\left[\sum_{\nu=L-1}^{L+1}\Pi^o(\kappa_A,\kappa_C,\nu)\Pi^o(\kappa_B,\kappa_D,\nu)\sum_{\mu=1}^{4}r_\mu^\nu(ABCD)R_\mu^\nu(ABCD)\right].\end{aligned} \tag{2.6}$$

The factor

$$\Pi^o(\kappa_A,\kappa_C,\nu) = \tfrac{1}{2}\left[1 + a_Aa_C(-1)^{j_A+j_C+\nu}\right] \tag{2.7}$$

is associated with the parity selection rule of the Gaunt interaction operator, which is opposite to the Coulomb parity selection rule. The values of a_A and a_C are $+1$ or -1, according to the positive or negative κ values, respectively. The coefficients $r_\mu^\nu(ABCD)$ and the radial integrals $R_\mu^\nu(ABCD)$ are presented in Tables I and II, respectively, for values of $\mu = 1$, 2, 3, or 4. For Table I, we have

$$P = \begin{cases} \frac{1}{L(2L-1)} & \text{for} \quad \nu = L-1, \\ -\frac{(\kappa_A+\kappa_C)(\kappa_B+\kappa_D)}{L(L+1)} & \text{for} \quad \nu = L, \\ \frac{1}{(L+1)(2L+3)} & \text{for} \quad \nu = L+1, \end{cases} \tag{2.8}$$

where $\overline{k} = \kappa_C - \kappa_A$ and $\overline{k'} = \kappa_D - \kappa_B$. $\frac{P_A(r)}{r}$ and $\frac{Q_A(r)}{r}$ are the large and small components of the radial part of the wave functions, respectively [7].

At the DF level, we need the knowledge of direct and exchange matrix elements of this operator, which are obtained by replacing $A = A$, $B = B$, $C = A$, and $D = B$ and $A = A$, $B = B$, $C = B$, and $D = A$, respectively [9]. However, the direct contribution to the Gaunt interaction is 0 [5]. So using the algebras of 3-j symbols from Ref. [9], we give the exchange matrix element of this operator as follows:

$$\begin{aligned}\langle A_1B_2|B_g|B_1A_2\rangle &= \sum_L(2j_B+1)\begin{pmatrix} j_A & L & j_B \\ \frac{1}{2} & 0 & -\frac{1}{2}\end{pmatrix}^2\left[\sum_{\nu=L-1}^{L+1}\Pi^o(\kappa_A,\kappa_B,\nu)\right. \\ &\quad\left.\times\sum_{\mu=1}^{4}r_\mu^\nu(ABBA)R_\mu^\nu(ABBA)\right].\end{aligned} \tag{2.9}$$

TABLE I. Coefficients $r_\mu^\nu(ABCD)$.

	$\nu = L-1$	$\nu = L$	$\nu = L+1$
$\mu = 1$	$P(L+\overline{k})(L+\overline{k'})$	P	$P(\overline{k}-L-1)(\overline{k'}-L-1)$
$\mu = 2$	$P(L-\overline{k})(L-\overline{k'})$	P	$P(\overline{k}+L+1)(\overline{k'}+L+1)$
$\mu = 3$	$P(L+\overline{k})(\overline{k'}-L)$	P	$P(\overline{k}-L-1)(\overline{k'}+L+1)$
$\mu = 4$	$P(\overline{k}-L)(L+\overline{k'})$	P	$P(\overline{k}+L+1)(\overline{k'}-L-1)$

TABLE II. Radial integrals $R^{\nu}_{\mu}(ABCD)$.

	$\nu = L-1, L$, or $L+1$
$\mu = 1$	$\int_0^\infty \int_0^\infty P_A(r_1)Q_C(r_1)V_\nu(1,2)P_B(r_2)Q_D(r_2)dr_1dr_2$
$\mu = 2$	$\int_0^\infty \int_0^\infty Q_A(r_1)P_C(r_1)V_\nu(1,2)Q_B(r_2)P_D(r_2)dr_1dr_2$
$\mu = 3$	$\int_0^\infty \int_0^\infty P_A(r_1)Q_C(r_1)V_\nu(1,2)Q_B(r_2)P_D(r_2)dr_1dr_2$
$\mu = 4$	$\int_0^\infty \int_0^\infty Q_A(r_1)P_C(r_1)V_\nu(1,2)P_B(r_2)Q_D(r_2)dr_1dr_2$

The coefficients $r^{\nu}_{\mu}(ABBA)$ are presented in Table III and the radial integrals $R^{\nu}_{\mu}(ABBA)$ are obtained from Table II by replacing $A = A$, $B = B$, $C = B$, and $D = A$. For Table III, we have

$$P = \begin{cases} \frac{1}{L(2L-1)} & \text{for} \quad \nu = L-1, \\ -\frac{(\kappa_A+\kappa_B)^2}{L(L+1)} & \text{for} \quad \nu = L, \\ \frac{1}{(L+1)(2L+3)} & \text{for} \quad \nu = L+1, \end{cases}$$

and $\overline{k} = -\overline{k'} = \kappa_B - \kappa_A$.

B. Coupled-cluster theory

The CC method is one of the most powerful highly correlated many-body methods, due to its all-order structure, to account for the correlation effects [35,36]. This method is used here for single-valance electron and has been described in detail elsewhere [31,35,37–41].

According to the CC theory, the correlated wave function of a single valance atomic state having valance orbital v is written in the form

$$|\Psi_v\rangle = e^T\{1 + S_v\}|\Phi_v\rangle. \tag{2.10}$$

Here, $|\Phi_v\rangle$ is the corresponding DF state. T is the closed-shell cluster operator, which considers excitations from the core orbitals, and S_v is the open-shell cluster operator corresponding to the valence electron v [41].

The correlated expectation value of an operator $\hat{O}$ at any particular atomic state Ψ_v can be written as

$$\begin{aligned} O^{\rm CC}_{vv} &= \frac{\langle\Psi_v|\hat{O}|\Psi_v\rangle}{\langle\Psi_v|\Psi_v\rangle} \\ &= \frac{\langle\Phi_v|\{1 + S^\dagger_v\}\overline{O}\{1 + S_v\}|\Phi_v\rangle}{\langle\Phi_v|\{1 + S^\dagger_v\}e^{T^\dagger}e^T\{1 + S_v\}|\Phi_v\rangle}, \end{aligned} \tag{2.11}$$

where $\overline{O} = e^{T^\dagger}Oe^T$.

TABLE III. Coefficients $r^{\nu}_{\mu}(ABBA)$.

	$\nu = L-1$	$\nu = L$	$\nu = L+1$
$\mu = 1$	$-P(\overline{k}^2 - L^2)$	P	$-P(\overline{k}^2 - (L+1)^2)$
$\mu = 2$	$-P(\overline{k}^2 - L^2)$	P	$-P(\overline{k}^2 - (L+1)^2)$
$\mu = 3$	$-P(\overline{k} + L)^2$	P	$-P(\overline{k} - (L+1))^2$
$\mu = 4$	$-P(\overline{k} - L)^2$	P	$-P(\overline{k} + (L+1))^2$

C. Hyperfine constant *A*

The hyperfine constant A of a state represented by $|JM\rangle$ is given by the following expression:

$$A = \mu_N g_I \frac{\langle J||\mathbf{T}^{(1)}||J\rangle}{\sqrt{J(J+1)(2J+1)}}, \tag{2.12}$$

where μ_N is the nuclear magneton and g_I is the g factor of the nucleus having nuclear spin I [41,42]. The operator $\mathbf{T}^{(1)}$ and the single-particle reduced matrix element of the electronic part of this operator is defined in Refs. [43,44].

III. RESULTS AND DISCUSSION

The CC calculations are based on the generation of the DF orbitals. Therefore, accurate description of the radial part of the orbital wave functions at the DF level is one of the building blocks of accurate calculations. Here, these orbitals are considered to be Gaussian-type orbitals and are generated in the environment of V^{N-1} potential of the Dirac-Coulomb Hamiltonian, where N is the number of electrons of each single-valance system [41]. The radial wave functions are generated on 750 grid points which follow $r_i = r_0[e^{h(i-1)} - 1]$, with $r_0 = 2 \times 10^{-6}$ and $h = 0.05$. The nuclei are considered to obey a Fermi-type distribution function [41]. The Gaussian-type orbitals are obtained by using the universal basis parameters: α_0 and β [41,42]. These parameters, presented in Table IV, are optimized for each system with respect to the wave functions obtained from the GRASP 2 code, where the DF equations are solved using a numerical technique [45].

In DF calculations, the number of basis functions is taken as 30, 25, and 20 for s, p, and d symmetries, respectively. However, in CC calculations, 12, 11, and 10 basis functions are used, including all the bound orbitals for s, p, and d symmetries, respectively. These numbers of symmetries and basis functions are chosen in accordance with the numerical convergence of the core correlation energies. In our discussions, the DF results are calculated for the Dirac-Coulomb Hamiltonian. Also, the correlation contributions ($\Delta^{\rm corr}$) are calculated by the differences between the CC and the DF results for the Dirac-Coulomb Hamiltonian, i.e., the Coulomb correlations. But the Gaunt contributions ($\Delta^{\rm Gaunt}$) are calculated by the differences between the CC results for the Dirac-Coulomb-Gaunt Hamiltonian and the Dirac-Coulomb Hamiltonian. The percentage correlation contributions ($\%\Delta^{\rm corr}$) and Gaunt contributions ($\%\Delta^{\rm Gaunt}$) are evaluated with respect to the DF results and CC results, respectively, for the Dirac-Coulomb Hamiltonian.

In Table V, the IPs at the DF level are presented along with the $\Delta^{\rm corr}$ and $\Delta^{\rm Gaunt}$. The total results are rounded off to the integer place and are compared with the results of NIST in the same table [30]. Our calculated IPs are presented within an approximate theoretical uncertainty of $\pm 0.03\%$ [46]. Except for Ca XVI, the final calculated IPs are in good agreement with the NIST results. However, our results for the former element are within the uncertainty limits (about $\pm 16\,000$ cm^{-1}) of the experimental measurements [4]. From Table V, one can see that the $\Delta^{\rm Gaunt}$ values are negative everywhere, and with increasing atomic number their absolute values increase monotonically, whereas the $\Delta^{\rm corr}$ values are

TABLE IV. Universal basis parameters: α_0 and β.

	Z													
	8	9	10	11	12	13	14	15	16	17	18	19	20	21
α_0	0.00225	0.00275	0.00325	0.00350	0.00425	0.00525	0.00625	0.00725	0.00825	0.00925	0.01025	0.01125	0.01225	0.01325
β	2.73	2.73	2.73	2.73	2.73	2.73	2.73	2.73	2.73	2.73	2.73	2.73	2.73	2.73

positive for lower atomic number and their values decrease with increasing Z and become negative at $Z \geqslant 17$ and $Z \geqslant 18$ for $2p\,^2P_{1/2}$ and $2p^2\,P_{3/2}$ states, respectively. According to Eliav *et al.*, for $Z = 10$, the estimated correlation contributions for $2p\,^2P_{1/2}$ and $2p\,^2P_{3/2}$ states are 4806.93 and 4865.75 cm^{-1}, respectively, where for $Z = 18$, these values are -1104.40 and -59.26 cm^{-1}, respectively which are in good agreement with our calculations. The IP of the $2p\,^2P_{3/2}$ state for $Z = 16$ calculated at the DF level is close to the total result. For this case, the absolute values of Δ^{Gaunt} and Δ^{corr} are relatively close to each other, but their signs are opposite. So the overall contribution of these two effects does not change the DF result significantly. However, the wave functions responsible for the DF and final results are different, which is observed in the calculations of the hyperfine constants as discussed later in the present paper.

As shown in Table V, at higher Z values, Δ^{Gaunt} values are comparable with Δ^{corr} values in determinations of IPs.

In Figs. 1 and 2, graphical variations of $\%\Delta^{\text{corr}}$ and $\%\Delta^{\text{Gaunt}}$ to the IPs w.r.t. Z are presented, respectively. The $\%\Delta^{\text{corr}}$ values initially decrease rapidly and then vary slowly, whereas absolute values of the $\%\Delta^{\text{Gaunt}}$ increase linearly with increasing Z. In Fig. 1, the $\%\Delta^{\text{corr}}$ curve of $2p\,^2P_{1/2}$ states shows slightly more fall compared to the curve of $2p\,^2P_{3/2}$ states. Even in Fig. 2, one can see that the curve of $2p\,^2P_{1/2}$ states is steeper than that of $2p\,^2P_{3/2}$ states. So from these two figures, it is obvious that with increasing Z, both $\%\Delta^{\text{Gaunt}}$ and $\%\Delta^{\text{corr}}$ are more effective for the former states than that of the latter states in determining the IPs. The correlation and Gaunt effects are found to vary from $+1$ to -0.1% and from -0.01% to -0.04%, respectively, in the IPs.

TABLE V. Calculated IPs with the correlation and Gaunt effects along with comparisons with the NIST results (in cm^{-1}).

Z	State	DF	Δ^{corr}	Δ^{Gaunt}	Total[a]	NIST[b]
8	$2p\,^2P_{1/2}$	618204.38	5808.89	−73.72	623940	624382
	$2p\,^2P_{3/2}$	617770.18	5803.55	−55.03	623519	623996
9	$2p\,^2P_{1/2}$	915988.05	5307.30	−128.55	921167	921430
	$2p\,^2P_{3/2}$	915158.69	5324.07	−98.90	920384	920686
10	$2p\,^2P_{1/2}$	1269209.36	4716.60	−204.62	1273721	1273820
	$2p\,^2P_{3/2}$	1267767.50	4764.47	−160.38	1272372	1272513
11	$2p\,^2P_{1/2}$	1677809.33	4060.48	−305.45	1681564	1681700
	$2p\,^2P_{3/2}$	1675470.31	4152.24	−242.35	1679380	1679565
12	$2p\,^2P_{1/2}$	2141817.07	3385.86	−433.87	2144769	2145100
	$2p\,^2P_{3/2}$	2138220.31	3536.45	−347.56	2141409	2141798
13	$2p\,^2P_{1/2}$	2661309.44	2677.04	−593.23	2663393	2662650
	$2p\,^2P_{3/2}$	2656009.14	2905.80	−478.73	2658436	2657760
14	$2p\,^2P_{1/2}$	3236356.19	1944.52	−787.29	3237513	3237300
	$2p\,^2P_{3/2}$	3228811.95	2274.68	−638.94	3230448	3230309
15	$2p\,^2P_{1/2}$	3867061.50	1193.76	−1019.32	3867236	3867100
	$2p\,^2P_{3/2}$	3856629.52	1651.45	−830.90	3857450	3857401
16	$2p\,^2P_{1/2}$	4553546.98	411.06	−1292.67	4552665	4552500
	$2p\,^2P_{3/2}$	4539468.86	1032.31	−1057.46	4539444	4539365
17	$2p\,^2P_{1/2}$	5295946.59	−371.31	−1610.97	5293964	5293800
	$2p\,^2P_{3/2}$	5277342.47	444.22	−1321.51	5276465	5276390
18	$2p\,^2P_{1/2}$	6094410.81	−1166.35	−1977.55	6091267	6090500
	$2p\,^2P_{3/2}$	6070267.99	−118.69	−1625.80	6068524	6067844
19	$2p\,^2P_{1/2}$	6949103.86	−1973.12	−2395.89	6944735	6943800
	$2p\,^2P_{3/2}$	6918267.32	−652.16	−1973.18	6915642	6914783
20	$2p\,^2P_{1/2}$	7860203.67	−2790.74	−2869.39	7854544	7860000
	$2p\,^2P_{3/2}$	7821366.32	−1152.48	−2366.49	7817847	7823480
21	$2p\,^2P_{1/2}$	8827901.77	−3618.45	−3401.58	8820882	8820000
	$2p\,^2P_{3/2}$	8779594.34	−1616.56	−2808.45	8775169	8774363

[a]Total = DF + Δ^{corr} + Δ^{Gaunt} (rounded off to the integer).

[b]NIST results [30].

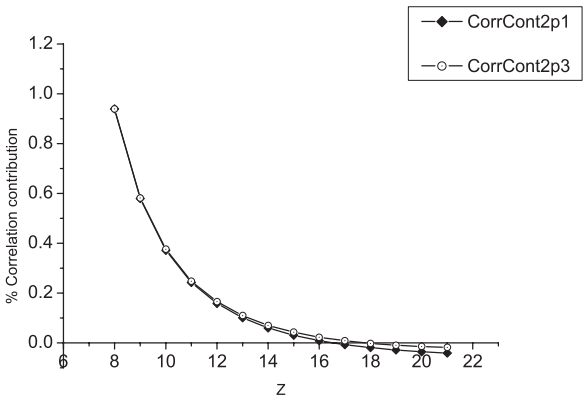

FIG. 1. Percentage correlation contributions (CorrCont) to IPs of $2p\,^2P_{1/2}$ (2p1) and $2p\,^2P_{3/2}$ (2p3) states.

In Table VI, the FSS between $2p\,^2P_{1/2}$ and $2p\,^2P_{3/2}$ states are tabulated with the correlation and Gaunt contributions. The final calculated results are compared with the results of NIST [30]. In this table one sees that, except at $Z = 8$, the $\Delta^{\rm corr}$ are negative for the rest of the Z values and their absolute values increase with increasing Z. But the $\Delta^{\rm Gaunt}$ are negative for all Z and their absolute values also increase with increasing Z. In the cases of Mg VIII, Si X, and S XII, our CC results (DF + $\Delta^{\rm corr}$) are in good agreement with the results of Nataraj *et al.* [25]. However, the significant improvement in the final results due to the inclusion of the Gaunt interaction, not only for these but also for other ions, is apparent in Table VI.

In Fig. 3, variations of the percentage correlation and Gaunt contributions to the FSS are plotted w.r.t. Z. This figure highlights that from $Z = 9$, absolute values of $\%\Delta^{\rm corr}$ first increase rapidly, then slow down, and, after $Z = 16$, decrease slowly, whereas absolute values of $\%\Delta^{\rm Gaunt}$ decrease systematically with increasing Z. Up to $Z = 9$, $\%\Delta^{\rm Gaunt}$ values dominate over $\%\Delta^{\rm corr}$, but after that the case is reversed. Figure 3 shows that the $\%\Delta^{\rm corr}$ vary from $+1.5$ to -4.5 and the $\%\Delta^{\rm Gaunt}$ vary from -4.5 to -1.5% in FSS. These show that both $\Delta^{\rm corr}$ and $\Delta^{\rm Gaunt}$ are very important in accurate determinations of FSS compared to IPs.

In Table VII, the hyperfine constants A are tabulated with the correlation and Gaunt effects. In these calculations, the most stable isotopes of each elements are chosen and the g_I values of these isotopes are calculated from Ref. [47]. Here we consider the g_I values, neglecting their signs. The multiconfiguration Dirac-Hartree-Fock results within the Breit-Pauli approximation of Jönsson *et al.* for O IV ($Z = 8$) of $2p\,^2P_{1/2}$ and $2p\,^2P_{3/2}$ states are 1647 and 324 MHz, respectively, which are in good agreement with our final results [28]. Table VII clearly shows that the correlation contributions arise as a dominating mechanism compared to the Gaunt contributions in determinations of hyperfine constants. Contrary to the IP, the DF result differs significantly from the final result for the $2p\,^2P_{3/2}$ state for $Z = 16$ due to the difference between the wave functions of the two levels of calculations.

The variation in $\%\Delta^{\rm corr}$, i.e., the percentage of total correlation contributions w.r.t. Z to the hyperfine constants, are shown in Figs. 4 and 5 for $2p\,^2P_{1/2}$ and $2p\,^2P_{3/2}$ states, respectively. Correlations for terms like the core correlation ($\overline{O}$-O), pair correlation ($\overline{O}S_{1v} + $c.c.), and lowest order core polarization ($\overline{O}S_{2v} + $c.c.) [42] are also plotted in the same figures. The percentage contributions from these terms are calculated w.r.t. the DF results. Like the IPs, here also

TABLE VI. Calculated FSS between $2p\,^2P_{1/2}$ and $2p\,^2P_{3/2}$ states with the correlation and Gaunt effects along with comparisons with the NIST results (in cm^{-1}).

Z	DF	$\Delta^{\rm corr}$	$\Delta^{\rm Gaunt}$	Total[a]	NIST[b]
8	434.20	5.34	−18.69	421	386
9	829.36	−16.77	−29.65	783	744
10	1441.86	−47.87	−44.24	1350	1307
11	2339.02	−91.76	−63.10	2184	2135
12	3596.76	−150.59	−86.31	3360	3302
13	5300.30	−228.76	−114.50	4957	4890
14	7544.24	−330.16	−148.33	7066	6991
15	10431.98	−457.69	−188.42	9786	9699
16	14078.12	−621.25	−235.21	13222	13135
17	18604.12	−815.53	−289.46	17499	17410
18	24142.82	−1047.66	−351.75	22743	22656
19	30836.54	−1320.96	−422.71	29093	29017
20	38837.35	−1638.26	−502.90	36696	36520
21	48307.43	−2001.89	−593.13	45712	45637

[a]Total = DF + $\Delta^{\rm corr}$ + $\Delta^{\rm Gaunt}$ (rounded off to the integer).
[b]NIST results [30].

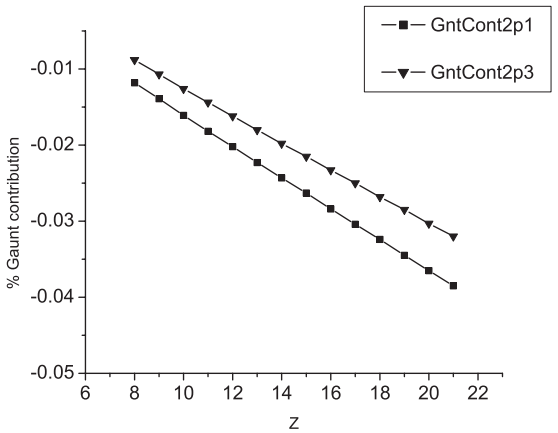

FIG. 2. Percentage Gaunt contributions (GntCont) to IPs of the $2p\,^2P_{1/2}$ (2p1) and $2p\,^2P_{3/2}$ (2p3) states.

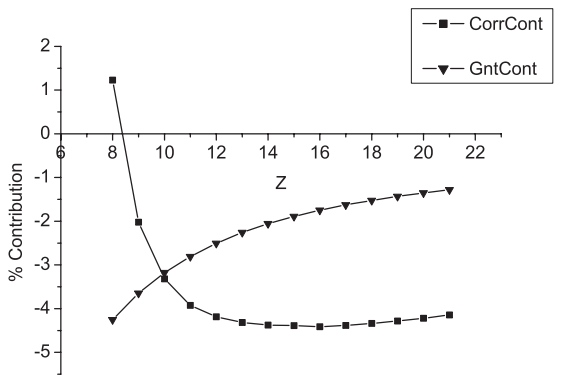

FIG. 3. Percentage correlation (CorrCont) and Gaunt (GntCont) contributions to FSS between $2p\,^2P_{1/2}$ and $2p\,^2P_{3/2}$ states.

TABLE VII. Calculated hyperfine constants A with the correlation and Gaunt effects (in MHz).

Z	g_I	State	DF	$\Delta^{\rm corr}$	$\Delta^{\rm Gaunt}$	Total[a]
8	0.7575	$2p\,^2P_{1/2}$	1595.69	64.98	0.03	1661
		$2p\,^2P_{3/2}$	317.67	25.37	−0.02	343
9	5.2577	$2p\,^2P_{1/2}$	18100.83	600.68	−0.10	18701
		$2p\,^2P_{3/2}$	3598.48	239.80	−0.29	3838
10	0.4412	$2p\,^2P_{1/2}$	2310.26	64.83	−0.05	2375
		$2p\,^2P_{3/2}$	458.56	26.97	−0.04	485
11	1.4784	$2p\,^2P_{1/2}$	11170.12	270.02	−0.49	11440
		$2p\,^2P_{3/2}$	2213.27	117.65	−0.26	2331
12	0.3422	$2p\,^2P_{1/2}$	3582.42	77.29	−0.20	3660
		$2p\,^2P_{3/2}$	708.45	35.37	−0.10	744
13	1.4566	$2p\,^2P_{1/2}$	20459.89	402.39	−1.42	20861
		$2p\,^2P_{3/2}$	4037.56	191.52	−0.65	4228
14	1.1106	$2p\,^2P_{1/2}$	20390.77	368.23	−1.68	20757
		$2p\,^2P_{3/2}$	4014.68	183.07	−0.75	4197
15	2.2632	$2p\,^2P_{1/2}$	53148.34	887.65	−5.15	54031
		$2p\,^2P_{3/2}$	10438.26	461.21	−2.23	10897
16	0.4292	$2p\,^2P_{1/2}$	12658.08	196.88	−1.41	12854
		$2p\,^2P_{3/2}$	2479.40	106.89	−0.60	2586
17	0.5479	$2p\,^2P_{1/2}$	19978.04	290.71	−2.54	20266
		$2p\,^2P_{3/2}$	3902.05	164.37	−1.05	4065
18	0.3714	$2p\,^2P_{1/2}$	16518.00	225.90	−2.37	16742
		$2p\,^2P_{3/2}$	3216.44	132.62	−0.96	3348
19	0.1433	$2p\,^2P_{1/2}$	7682.31	99.13	−1.23	7780
		$2p\,^2P_{3/2}$	1491.10	60.23	−0.49	1551
20	0.3765	$2p\,^2P_{1/2}$	24077.93	294.13	−4.29	24368
		$2p\,^2P_{3/2}$	4657.46	184.30	−1.68	4840
21	1.3590	$2p\,^2P_{1/2}$	102723.90	1191.39	−20.18	103895
		$2p\,^2P_{3/2}$	19798.50	767.11	−7.75	20558

[a]Total = DF + $\Delta^{\rm corr}$ + $\Delta^{\rm Gaunt}$ (rounded off to the integer).

the $\%\Delta^{\rm corr}$ first decrease rapidly and then decrease slowly with increasing Z. But unlike the IPs, the $\%\Delta^{\rm corr}$ are positive everywhere. The $\%\Delta^{\rm corr}$ of $2p\,^2P_{1/2}$ and $2p\,^2P_{3/2}$ states vary from +4.25 to +1.25% and from +8 to +4%, respectively. The pair correlation effects are positive, but the core correlation and core polarization effects are opposite in sign between the fine structure states. As Z increases, absolute values of the percentage correlation contributions from the different correlation terms decrease. Among these, the core correlation effects are the most stable with respect to the other two correlation effects. At higher Z values, major correlations come from the core correlations and the next-highest contributions come from the core polarizations. The correlation contributions from the term $S^{\dagger}_{2v}\overline{O}S_{2v}$ + c.c., which are not shown in Figs. 4 and 5

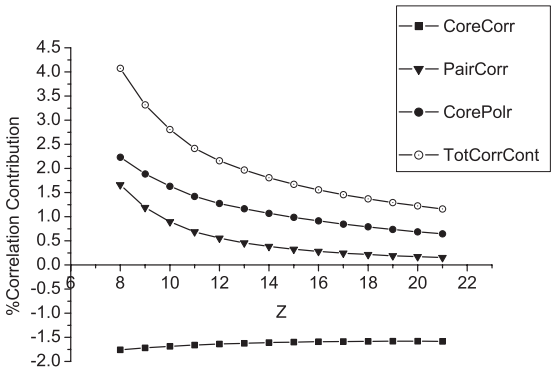

FIG. 4. Percentage of total correlation contributions (TotCorrCont) with core correlation (CoreCorr), pair correlation (PairCorr), and core polarization (CorePolr) effects in the hyperfine constants A of $2p\,^2P_{1/2}$ states.

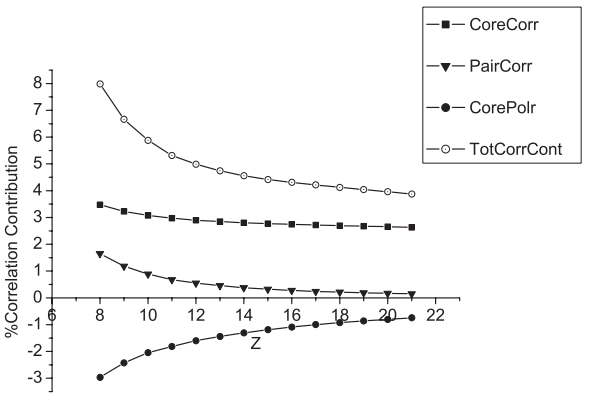

FIG. 5. Percentage of total correlation contributions (TotCorrCont) with core correlation (CoreCorr), pair correlation (PairCorr), and core polarization (CorePolr) effects in the hyperfine constants A of $2p^2P_{3/2}$ states.

TABLE VIII. Correlation effects in the Gaunt contributions to IPs (ΔE_g^I; in cm^{-1}), FSS (ΔE_g^F; in cm^{-1}), and hyperfine constants A (ΔA_g; in MHz).

Z	State	ΔE_g^I	ΔE_g^F	ΔA_g
8	$2p\,^2P_{1/2}$	5.98		1.04
	$2p\,^2P_{3/2}$	2.13	3.85	0.16
9	$2p\,^2P_{1/2}$	9.29		12.88
	$2p\,^2P_{3/2}$	3.07	6.22	2.01
10	$2p\,^2P_{1/2}$	13.12		1.81
	$2p\,^2P_{3/2}$	3.99	9.13	0.29
11	$2p\,^2P_{1/2}$	17.59		9.43
	$2p\,^2P_{3/2}$	4.82	12.77	1.52
12	$2p\,^2P_{1/2}$	22.83		3.28
	$2p\,^2P_{3/2}$	5.54	17.29	0.53
13	$2p\,^2P_{1/2}$	28.91		20.22
	$2p\,^2P_{3/2}$	6.19	22.72	3.25
14	$2p\,^2P_{1/2}$	35.61		21.60
	$2p\,^2P_{3/2}$	6.51	29.12	3.45
15	$2p\,^2P_{1/2}$	42.60		60.00
	$2p\,^2P_{3/2}$	6.52	36.08	9.52
16	$2p\,^2P_{1/2}$	51.34		15.16
	$2p\,^2P_{3/2}$	6.18	45.16	2.39
17	$2p\,^2P_{1/2}$	60.22		25.28
	$2p\,^2P_{3/2}$	5.39	54.83	3.97
18	$2p\,^2P_{1/2}$	69.81		22.01
	$2p\,^2P_{3/2}$	4.15	65.66	3.43
19	$2p\,^2P_{1/2}$	80.19		10.74
	$2p\,^2P_{3/2}$	2.42	77.77	1.66
20	$2p\,^2P_{1/2}$	91.31		35.23
	$2p\,^2P_{3/2}$	0.12	91.19	5.42
21	$2p\,^2P_{1/2}$	103.10		156.90
	$2p\,^2P_{3/2}$	−2.68	105.78	24.03

are also significant in the $2p\,^2P_{3/2}$ states of the lower Z members. For these states, this term contributes from +4.82% to +0.43% with increasing Z. However, for $2p\,^2P_{1/2}$ states its contribution varies from +0.85 to +0.11% as Z increases. The remaining correlation contributions come from other terms like $S_{1v}^{\dagger}\overline{O}S_{1v}$ + c.c., $S_{1v}^{\dagger}\overline{O}S_{2v}$ + c.c., other effective two-body terms, and normalization corrections [42].

In Table VIII, correlation effects in the Gaunt contributions, i.e., the differences in the Gaunt contributions from the CC to the DF levels, to the IPs, FSS, and hyperfine A constants, are presented. In the IPs, it is seen that for $2p\,^2P_{1/2}$ states the correlation effects in the Gaunt contributions increase systematically, and for $2p\,^2P_{3/2}$ states, they increase up to $Z = 15$ and then start decreasing with increasing Z. Also, for these properties, these effects are relatively stronger for $2p\,^2P_{1/2}$ states compared to $2p\,^2P_{3/2}$ states. In the IPs, the correlation effects change the Gaunt contributions from the DF to the CC levels by +7.50% to +2.94% and by +3.73 to −0.09% for $2p\,^2P_{1/2}$ and $2p\,^2P_{3/2}$ states, respectively. However, in the FSS, the changes are stronger, at are about +17.34 to +15.13%. As expected, due to the relatively large correlation effects, dramatic changes occur in the hyperfine constants, which almost exhaust the Gaunt contributions at the DF levels and provide very little at the CC levels. These changes are about +102.97 to +88.60% and about +88.89 to +75.61% for $2p\,^2P_{1/2}$ and $2p\,^2P_{3/2}$ states, respectively.

IV. CONCLUSION

Detailed analysis of the electron correlation and Gaunt contributions to IPs and hyperfine constants A have been performed for the first two low-lying states of boron-like systems using the RCC approach. We have reported the important role of these two effects in determinations of the FSS. Gaunt contributions from the DF to the CC levels of calculations have been discussed extensively. The strengths of the correlation and Gaunt effects among all these properties with increasing Z have been established. In the framework of the RCC theory, contributions from the different important correlation terms to the hyperfine constants A have been studied descriptively. We hope that, in future, our study will be extended to incorporate the retardation as well as the QED effects at both the DF and the CC levels of calculations for more accurate descriptions of all these properties. This will also be useful to judge the relative strengths of all these effects with increasing Z, not only for this sequence but also for all the other isoelectronic sequences having a higher degree of correlation.

ACKNOWLEDGMENTS

We are grateful to Professor B. P. Das and Dr. R. K. Chaudhuri, Indian Institute of Astrophysics, Bangalore, and Dr. B. K. Sahoo, Physical Research Laboratory, Ahmedabad, India, for providing the CC and HYPERFINE code in which we implemented the Gaunt interaction. We are very thankful to Dr. A. D. K. Singh and Mr. B. K. Mani, Physical Research Laboratory, Ahmedabad, India, for valuable suggestions regarding implementation of the Gaunt interaction in the CC code. We appreciate the help of Dr. G. Dixit, Center for Free-Electron Laser Science, Hamburg, Germany. We would like to recognize the funding support from the Council of Scientific and Industrial Research (CSIR), India.

[1] K. Pachucki and V. A. Yerokhin, Phys. Rev. Lett. **104**, 070403 (2010).
[2] V. A. Yerokhin, A. N. Artemyev, and V. M. Shabaev, Phys. Rev. A **75**, 062501 (2007).
[3] L. H. Hao and G. Jiang, Phys. Rev. A **83**, 012511 (2011).
[4] H. Jie, Z. Qian, and J. Gang, Commun. Theor. Phys. **54**, 871 (2010).
[5] J. B. Mann and W. R. Johnson, Phys. Rev. A **4**, 41 (1971).
[6] Y. K. Kim, Phys. Rev. **154**, 17 (1967).
[7] I. P. Grant and N. C. Pyper, J. Phys. B **9**, 761 (1976).
[8] M. Reiher and J. Hinze, J. Phys. B **32**, 5489 (1999).
[9] I. P. Grant, *Relativistic Quantum Theory of Atoms and Molecules, Theory and Computation, Springer Series on Atomic, Optical and Plasma Physics 40* (Springer, Berlin, 2007).
[10] P. Bogdanovich, R. Karpuškiene, and O. Rancova, Phys. Scripta **75**, 669 (2007).
[11] J. Li, P. Jönsson, C. Dong, and G. Gaigalas, J. Phys. B **43**, 035005 (2010).
[12] H. L. Zhang and D. H. Sampson, At. Data Nucl. Data Tables **56**, 41 (1994).
[13] K. Koc, J. Phys. B **36**, L93 (2003).
[14] K. Koc, Nucl. Instrum. Methods Phys. Res. Sec. B **235**, 46 (2005).
[15] K. Koc, Phys. Scripta **67**, 491 (2003).
[16] K. Koc, Eur. Phys. J. D **53**, 9 (2009).
[17] G. Tachiev and C. F. Fischer, J. Phys. B **33**, 2419 (2000).
[18] U. I. Safronova, W. R. Johnson, and A. E. Livingston, Phys. Rev. A **60**, 996 (1999).
[19] M. S. Safronova, W. R. Johnson, and U. I. Safronova, Phys. Rev. A **54**, 2850 (1996).
[20] U. I. Safronova, W. R. Johnson, and M. S. Safronova, At. Data Nucl. Data Tables **69**, 183 (1998).
[21] G. Merkelis, M. J. Vilkas, G. Gaigalas, and R. Kisielius, Phys. Scripta **51**, 233 (1995).
[22] M. E. Galavis, C. Mendoza, and C. J. Zeippen, Astron. Astrophys. Suppl. Ser. **131**, 499 (1998).
[23] N. W. Zheng and T. Wang, Int. J. Quantum Chem. **98**, 495 (2004).
[24] E. Eliav, U. Kaldor, and Y. Ishikawa, Chem. Phys. Lett. **222**, 82 (1994).
[25] H. S. Nataraj, B. K. Sahoo, B. P. Das, R. K. Chaudhuri, and D. Mukherjee, J. Phys. B **40**, 3153 (2007).
[26] E. Eliav, U. Kaldor, and Y. Ishikawa, Phys. Rev. A **49**, 1724 (1994); **51**, 225 (1995).
[27] S. N. Panigrahy, R. W. Dougherty, T. P. Das, and J. Andriessen, Phys. Rev. A **40**, 1765 (1989).

[28] P. Jönsson, J. Li, G. Gaigalas, and C. Dong, At. Data Nucl. Data Tables **96**, 271 (2010).
[29] N. S. Oreshkina, D. A. Glazov, A. V. Volotka, V. M. Shabaev, I. I. Tupitsyn, and G. Plunien, Phys. Lett. A **372**, 675 (2008).
[30] Y. Ralchanko, A. E. Kramida, J. Reader, and NIST ASD TEAM, *NIST Atomic Spectra Database*, version 4.1.0 (2011); available at: [http://physics.nist.gov/asd3].
[31] G. Dixit, B. K. Sahoo, R. K. Chaudhuri, and S. Majumder, Phys. Rev. A **76**, 042505 (2007).
[32] G. Breit, Phys. Rev. **34**, 553 (1929); **36**, 383 (1930); **39**, 616 (1932).
[33] M. Reiher and B. A. Hess, *Relativistic Electronic-Structure Calculations for Atoms and Molecules*, Modern Methods Algorithms Quantum Chem., NIC Series, Vol. 3, edited by J. Grotendorst (John von Neumann Institute for Computing, Jülich, 2000), p. 479.
[34] J. A. Gaunt, Proc. R. Soc. London A **122**, 513 (1929).
[35] I. Lindgren and J. Morrison, *Atomic Many-Body Theory*, Vol. 3, edited by G. E. Lambropoulos and H. Walther (Berlin, Springer, 1985).
[36] N. N. Dutta and S. Majumder, Astrophys. J. **737**, 25 (2011).
[37] I. Lindgren and D. Mukherjee, Phys. Rep. **151**, 93 (1987).
[38] A. Haque and D. Mukherjee, J. Chem. Phys. **80**, 5058 (1984).
[39] S. Pal, M. Rittby, R. J. Bartlett, D. Sinha, and D. Mukherjee, Chem. Phys. Lett. **137**, 273 (1987); J. Chem. Phys. **88**, 4357 (1988).
[40] K. Raghavachari, G. W. Trucks, J. A. Pople, and M. Head-Gordon, Chem. Phys. Lett. **157**, 479 (1989); M. Urban, J. Noga, S. J. Cole, and R. J. Bartlett, *ibid*. **83**, 4041 (1985).
[41] B. K. Sahoo, R. K. Chaudhuri, B. P. Das, H. Merlitz, and D. Mukherjee, Phys. Rev. A **72**, 032507 (2005).
[42] G. Dixit, H. S. Nataraj, B. K. Sahoo, R. K. Chaudhuri, and S. Majumder, Phys. Rev. A **77**, 012718 (2008).
[43] B. K. Sahoo, R. K. Chaudhuri, B. P. Das, S. Majumder, H. Merlitz, U. S. Mahapatra, and D. Mukherjee, J. Phys. B **36**, 1899 (2003).
[44] R. K. Chaudhuri and K. F. Freed, J. Chem. Phys. **122**, 204111 (2005).
[45] F. A. Parpia, C. F. Fischer, and I. P. Grant, Comput. Phys. Commun. **175**, 745 (2006).
[46] The Editors, Phys. Rev. A **83**, 040001 (2011).
[47] P. Raghavan, At. Data Nucl. Data Tables **42**, 189 (1989).